Research Article

International Journal of Petrochemistry & Natural Gas

Fes Encapsulated Chitosan-G-Polyacrylamide Nanocomposite For The Removal Of Model Anionic Eosin Y From Water: Isotherm, Kinetics And Equilibrium Studies

Bernice Y.Danu[1], Eric S. Agorku[2], Francis K. Ampong[3], Johannes A.M. Awudza[2], Vincent Torve[2], Caleb Amponsah[3], Ruth N.M Quaye[3], Onoyivwe A. Monday[4,5,6], Peter O. Osifo[4], Suprakas S. Ray[5,6]

[1]*Department of Chemical Sciences, University of Energy and Natural Resources, P.O.Box 214, Sunyani, Ghana.*

[2]*Department of Chemistry, Kwame Nkrumah University of Science and Technology, PMB, Kumasi, Ghana.*

[3]*Department of Physics, Kwame Nkrumah University of Science and Technology, PMB, Kumasi, Ghana.*

[4]*Department of Chemical Engineering, Vaal University of Technology, Private Mail Bag X021, Vanderbijlpark 1900, South Africa.*

[5]*Department of Chemical Science, University of Johannesburg, Doornfontein, 2028, Johannesburg, South Africa.*

[6]*DST-CSIR National Center for Nanostructured Materials, Council for Scientific and Industrial Research, Pretoria 0001, South Africa*

***Corresponding author**

Eric S. Agorku, Department of Chemistry, Kwame Nkrumah University of Science and Technology, PMB, Kumasi, Ghana.

Submitted: 13 Apr 2022; **Accepted:** 19 Apr 2022; **Published:** 30 Apr 2022

Citation: *Bernice Y.Danu, Eric S. Agorku, Francis K. Ampong, Johannes A.M. Awudza, Vincent Torve, Caleb Amponsah, Ruth N.M Quaye, Onoyivwe A. Monday , Peter O. Osifo, Suprakas S. Ray .(2022). Fes Encapsulated Chitosan-G-Polyacrylamide Nanocomposite For The Removal Of Model Anionic Eosin Y From Water: Isotherm, Kinetics And Equilibrium Studies.Int J Petro Chem Natur Gas, 2(1):30-38.*

Abstract

A novel bio-nanocomposite, FeS/chitosan grafted polyacrylamide, was successfully synthesized by means of a grafting technique that employs microwave irradiation. Employing FTIR, SEM, XRD, TEM and SAED analysis, the synthesized nanocomposites were characterized. Thermodynamic and kinetic studies were performed using the batch mode via the adsorption of eosin yellow from aqueous solution using the nanocomposite. The adsorption process was tailored to the pseudo-second order kinetic model and the Freundlich isotherm model. The enthalpy change, ΔH° (-12.243 kJ/mol), was an exothermic process. The Gibbs energy, ΔG° (from -5.492 kJ/mol.K to -5.078 kJ/mol.K for temperatures from 300 K to 318 K respectively) values were indications of a thermodynamically feasible reaction process which was spontaneous within the temperature domain. The change in entropy, ΔS° (-0.023 kJ/mol), showed a reduced randomness during the adsorption process. The mean free energy of adsorption was 0.408 kJ/mol, which was an indication of physisorption. These results show the possible use of the graft copolymer as an adsorbent in water treatment.

Keywords: Keywords: Grafting; Chitosan-g-acrylamide; Iron sulphide; pseudo-second-order kinetics; Freundlich isotherm

Introduction

Water pollution due to the discharge of effluents from industries is of critical concern owing to its hazardous nature and threat it poses to humans and environment. A major industry that contributes to the release of these effluents is the textile and dyeing industry. Textile and dyeing industries utilize a generous amount of water during manufacturing and employ toxic colorants such as dyes in colouring of their final products. Consequently, they are considered one of the largest generators of contaminated wastewater [1-5].Owing to the complexity of the aromatic structure of most dyes, it is an arduous task to remedy these pollutants since they are stable to light and heat and non- biodegradable [6]. Various remediation techniques which include chemical oxidation, electrocoagulation, coagulation, anaerobic and aerobic microbial degradation, membrane separation and adsorption have been investigated extensively for the uptake of dyes from contaminated effluents [7-8]. Conversely, adsorption has demonstrated to be an economical and effectual means of treating dye effluents, because it gives off high-

ly treated effluents. Several suitable low-cost adsorbents, namely peat, silica, bentonite, fly ash, wood shavings and maize cob have been employed in wastewater treatments but these adsorbents generally have low removal rate thus large magnitude are needed for the complete treatment of dye effluents [9]. Recently, attention has been concentrated on biomaterials for dye removal owing to their advantage over synthetic polymers. These biomaterials are biodegradable, low cost and easily available[10]. Another advantage is that they do not leave residues of the by-products and can easily be isolated after the adsorption process is completed [10-12]. Despite these advantages, biopolymer-based adsorbents have poor mechanical strength and water solubility as compared to synthetic polymers. It is therefore necessary to improve their strength and stability by modifying its properties by graft copolymerization and the incorporation of nanoparticles [13,14]. Nanoparticle based adsorbents have drawn significant attention because of unique properties such as very small size and high surface area to volume ratio [15,16]. Incorporation of these nanoparticles within the polymer matrix not only increase the surface area but also provides additional properties for the binding of dye molecules [17]. Graft copolymerization is the method in which one or more polymers are covalently bonded to the polymer backbone of another polymer [18].

Chitosan is known to be a bio-compatible, bio- degradable, bio-inexhaustible, nontoxic polymer and the second most bounteous regular polysaccharide after cellulose known to mankind. It is obtained from the deacetylation of chitin which takes place in the exoskeleton of insects, crustacean shells, shrimps, prawns as well as the cell walls of fungi [19,20]. Due to its amine and hydroxyl functional groups, it can attract the alkyl, acetyl, sulphonyl and carboxylic groups in dyes [21,22]. Acrylamide is a receptive compound utilized as a monomer for the amalgamation of polyacrylamide. Owing to its high-water retention capacity, it has been utilized in wastewater treatment and drug delivery [23].

In this work, chitosan was modified by microwave- assisted grafting of polyacrylamide followed by the dispersion of FeS nanoparticles for the adsorption of Eosin yellow from aqueous solutions. Experimental adsorption isotherms, kinetics data and thermodynamic properties were analysed using different adsorption models.

Materials And Methods

All chemicals used were of analytical grade and used without further treatment. Glycerol, FeSO4 .7H2O, Na2S, ethanol, eosin yellow (EY), chitosan, acrylamide and acetic acid were obtained from Merck Limited.

Synthesis Of Fes Nanoparticle

Hundred (100) ml of aqueous 0.5 M of $FeSO_4.7H_2O$ and 2 ml of glycerol were added together with vigorous stirring under N_2 gas. 100 ml of Na2S aqueous solution under continuous stirring was added dropwise to the mixture until a colour change was observed from pale green to brick brown and finally to dark green. This was stirred for about 20 minutes and washed with distilled water and ethanol repeatedly. The final product was then dried in a hot air oven at 333 K overnight. Dried FeS was ground into powder and stored for further application.

Synthesis Of Fes/Chitosan Graft Poly(Acrylamide) Nanocomposite

Two (2) g of chitosan was dissolved in 100 ml 1% acetic acid and added dropwise to 50 ml acrylamide (0.1 M) solution with continuous stirring. An appropriate amount of FeS was added into the reaction mixture while stirring for about 45 minutes. The resultant mixture was placed in a microwave reactor at 333 K for 15- 20 minutes at 15 psi pressure [23]. The product was washed copiously with deionized water to remove any homopolymer formed during the reaction. The final product was dried at 333 K in a hot air oven overnight, after which it was ground to powder and stored for future application.

Adsorption Studies

A stock solution of EY was prepared by dissolving 0.3 g in 1 L of deionized water. Using serial dilution, subsequent solutions required for the adsorption tests were prepared from the stock solution.

Effect Of Adsorption Conditions

Using batch adsorption experiments, various parameters were determined by agitating a desired amount of the composite with the dye solutions (50 ml) of desired concentration and pH on a mechanical shaker at an agitation speed of 150 rpm. Contact time was varied at 10, 20, 30, 40, 50, 60, 70, 80, and 90 minutes. For loading (adsorbent dose), FeS/chitosan-g-poly(acrylamide) nanocomposite (0.05, 0.1, 0.15, 0.20, 0.25, 0.30, 0.35 and 0.40 g) was agitated with 50 ml dye solution at constant concentration and temperature for 120 minutes. Five (5) initial concentrations for EY (60, 80, 100, 120, 150 mg/L) were utilized for the study of the effect of initial concentration on adsorption at 300 K for 2 hours. The pH (2, 4, 6, 8, 10) was also varied using 0.1 M NaOH and 0.1 M HCl solutions. The impact of temperature was studied at different temperatures (300, 303, 308, 313, and 318 K) using 50 ml solutions of 100 mg/L in a MaxQ 8000 incubator stackable shaker. The residual EY concentrations in aqueous solutions were measured using a Shidmazu UV-Vis spectrophotometer at absorbance of 516 nm. The amount of dye adsorbed, Qe, or R.E were calculated as follows:

$$R.E = \frac{C_o - C_e}{C_o} \times 100 \quad (1)$$

where C_o is the initial dye concentration (mg/L), Ce is the final dye concentration at equilibrium (mg/L) and,

$$Q_e\,(mg/g) = \frac{C_o - C_e}{M} \times V \quad (2)$$

where C_o is the initial dye concentration (mg/L), Ce is the final dye concentration at equilibrium (mg/L), M is the mass of the adsorbent (g) and V is the volume of the dye solution (L).

Adsorption Isotherms

Adsorption isotherms portray the behaviour of the interaction between the adsorbent and the adsorbate molecules at equilibrium. The data obtained was tested using the Langmuir, Freundlich and Dubinin-Radushkevich adsorption isotherm models. These isotherm models can be used to describe the equilibrium characteristics of adsorption.

The Langmuir isotherm (Langmuir, 1916) assumes that there is a homogeneous dispersion of active adsorption sites on the adsorbent surface which absorbs a single layer adsorbate molecule with no interaction between the adsorbed molecules. The Langmuir isotherm equation is described by the equation;

$$Q_e = \frac{Q_m K_L C_e}{1+K_L C_e} \quad (3)$$

where C_e (mg/L) is the liquid phase concentration at equilibrium and Q_e (mg/g) is the mass of the dye concentration absorbed per unit mass. A graph of 1/Qe versus $1/C_e$ was plotted.

The Freundlich model assumes that with an increment in adsorbate concentration, the concentration of the adsorbate on the adsorbent surface also builds, corresponding to exponential decreases in adsorption energy after all the adsorption centers on the adsorbent are occupied [24]. The expression for this model is given as;

$$Log\ Q_e = \frac{1}{n} logC_e + logK_F \quad (4)$$

where Q_e is the amount of adsorbate adsorbed per unit mass (mg/g), C_e is the equilibrium concentration of the adsorbate (mg/L) and K_F (mg/g)(L/mg)$^{1/n}$ and 1/n are constants representing the adsorbent capacity and the heterogeneity factor, respectively. The value of 1/n must be greater than zero but lesser than unity for any adsorption to be favourable.

The Dubinin-Radushkevich isotherm describes whether the adsorption was physical or chemical [25]. This is described by the equation;

$$\ln q_e = \ln q_{DR} - \beta\varepsilon^2 \quad (5)$$

where q_{DR} (mg/g) is the Dubinin-Radushkevich maximum monolayer adsorption capacity, β (mol^2/J^2) is activity coefficient related to mean adsorption energy, and ε is the Polanyi potential which is calculated using the relationship

$$\varepsilon = RT \ln(1 + \frac{1}{C_e}) \quad (6)$$

where R (8.314 J/mol K) is the gas constant, T (K) is temperature and C_e (mg/L) is the concentration of adsorbate at equilibrium.

Characterization

The morphology of the nanocomposite and the grafted copolymer were obtained using SEM and TEM. Selective area electron diffraction (SAED) analysis was obtained from the TEM. XRD was used for the identification of the crystal structure of the materials. FTIR was used to determine the functional groups and the chemical bonds present in the materials.

Results And Discussion

FTIR Analysis

The FTIR spectra of FeS NP and FeS/chitosan-g-poly(acrylamide) nanocomposite are shown in Fig 1 (a, b). Fig 1a showed a broad peak at 3332 cm^{-1} attributed to O-H vibrations from water molecules absorbed by the sample. Peaks at 1632 cm^{-1} and 621 cm^{-1} were as a result of S-S vibrational stretch from the FeS nanoparticle [26]. A peak at 1133 cm^{-1} was characteristic of the S-O stretching vibration. In the fingerprint region, vibration bands corresponding to Fe-S stretch were observed below 500 cm^{-1} [27]. The FTIR of the grafted nanocomposite (Fig 1b) showed a broad absorption band at 3188 cm^{-1} which was due to overlapping of O-H stretching of chitosan and N-H stretching of amide groups. A peak at 1543 cm^{-1} was due to the carbonyl (C=O) stretching of secondary amide [1,28]. A band at 1401 cm^{-1} was due to C-N vibrational stretch which was an indication of the grafting between chitosan and polyacrylamide [1] Peaks found below 500 cm^{-1} were as a result of Fe-S stretching mode [23,27]. The shift in peak positions of Fe-S bands indicated the interaction of the copolymer with the nanocomposite.

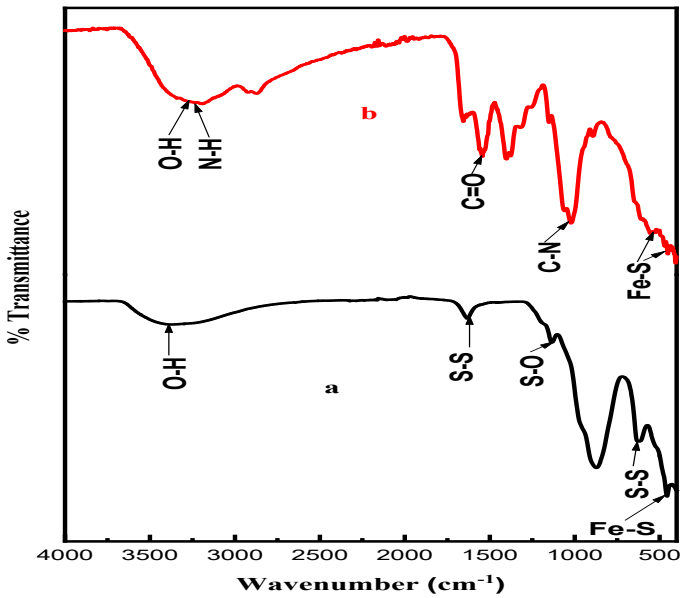

Figure 1: FTIR spectra of FeS NP (a) and FeS/chitosan-g-poly(acrylamide) nanocomposite

(b).3.2. Xrd Analysis

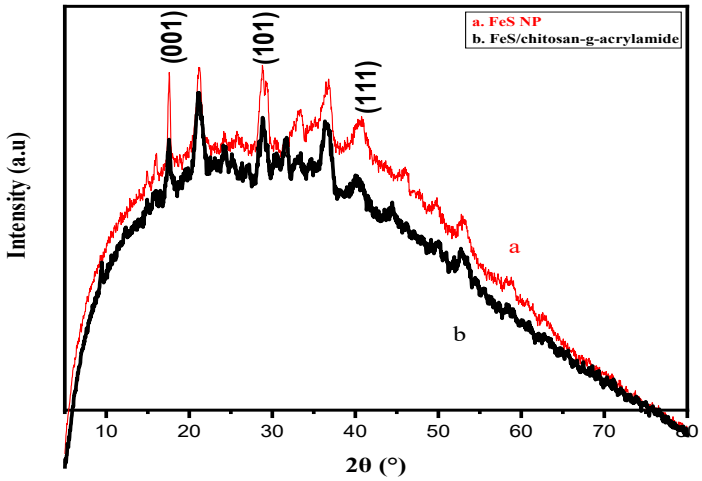

Figure 2: XRD patterns of FeS NP (a) and FeS/chitosan-g-poly(acrylamide) nanocomposite (b).

Fig 2 shows the XRD patterns of the as-synthesized FeS NP and FeS/chitosan-g- poly(acrylamide) nanocomposite. The peak positions (2θ values) at 17.56º, 28.83º and 40.75º corresponded to reflections from the (001), (101) and (111) planes of the tetragonal FeS phase (JCPDS: 86-0389) [27]. The grafted nanocomposite showed lower intensity in the peaks as compared to the FeS NP. This may be due to the interaction of the polymers (chitosan and polyacrylamide) with the nanoparticle and the less crystalline nature of the nanocomposite, compared to the nanoparticle [28]. From the Sherrer equation, the crystallite size of the FeS nanoparticle was found to be 6.2 nm.

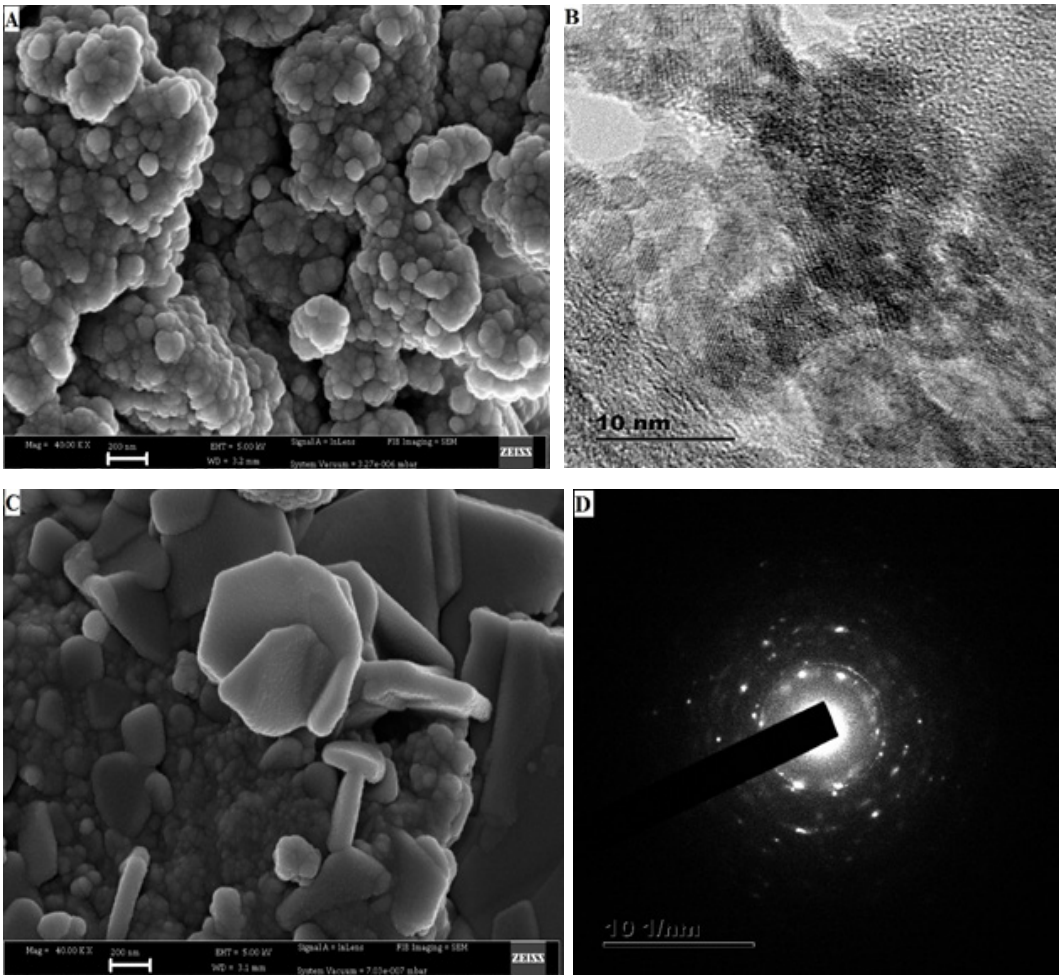

Figure 3: SEM image of FeS NP (A), TEM image of FeS NP (B), SEM image of FeS/chitosan-g-poly(acrylamide) nanocomposite (C), SAED pattern of FeS NP (D).

(Fig 3 A, B) shows the SEM and TEM micrographs of the as- synthesized FeS nanoparticle. The as-synthesized FeS nanoparticles were seen to be agglomerated and spherical or globular shaped. FeS NP synthesized through the conventional methods, tend to agglomerate rapidly to macroparticles due to the interparticle van der Waals interaction [29]. Similar spherical shaped results were reported by other researchers [30-32] (Fig 3 C, D shows SEM image of FeS/chitosan-g-poly(acrylamide) nanocomposite and the SAED pattern of FeS NP obtained from the TEM microscope respectively. The SEM of the graft nanocomposite revealed that FeS NP was coated by the copolymer. The flake- like appearance was due to the grafting of FeS and polymers (chitosan and acrylamide) (Pathania et al., 2016). Though not all of the chitosan and acrylamide was fully grafted.

The SAED pattern of FeS (Fig 3D) showed small spots forming rings ascribed to the Bragg reflections from the individual crystallite of the FeS nanoparticle indicating polycrystalline nature of the particles [28].

Adsorption Removal Experiments

Effect of EY concentration and FeS/chitosan-g-poly(acrylamide) dosage

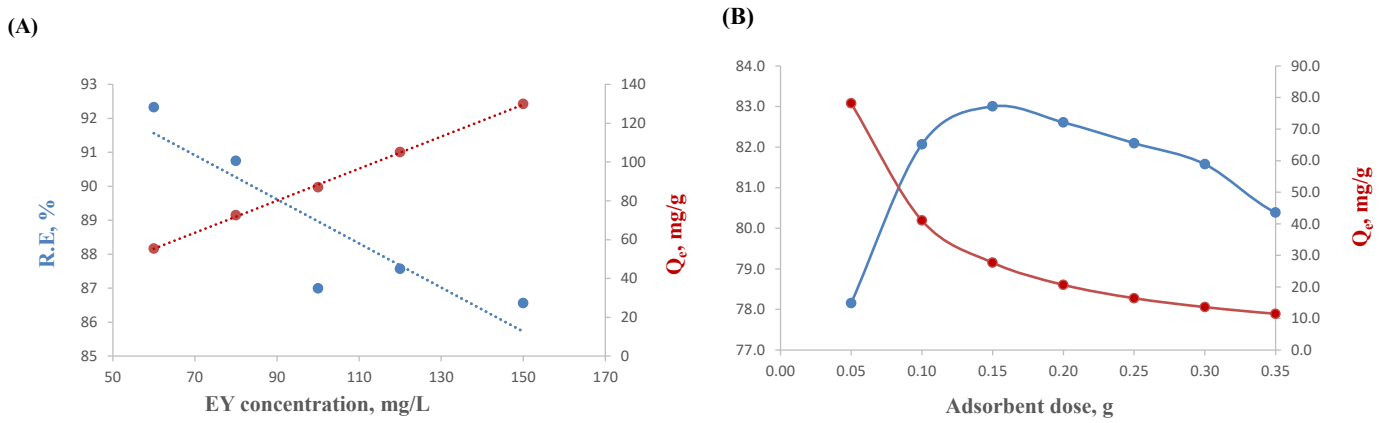

Figure 4: Effect of concentration (A) and dosage (B) on EY adsorption onto FeS/chitosan-g-poly(acrylamide) nanocomposite. Conditions: (A. temperature: 300 K; time: 120 minutes; dose; 0.05 g/50 ml) (B. temperature: 300 K; Time: 120 minutes; concentration: 100 mg/L).

From the graph above (Fig 4A), the removal efficiency decreased from 92.32% to 86.56% with an increase in EY concentration. However, the amount of dye adsorbed per unit mass of the adsorbent increased from 55.39 mg/g to 129.84 mg/g with increase in EY concentration. The decrease in R.E may be due to fewer number of available surface-active sites as the concentration increased. The increase in Qe may be attributed to a large mass transfer driving force. At lower concentration, fewer adsorbate particles are attached to the surface of the FeS/chitosan-g-poly(acrylamide) nanocomposite but as the concentration increased, the mass transfer driving force towards the adsorbent surface increased.

Fig 4B shows the effect of adsorbent dose on the adsorption of EY onto FeS/chitosan-g- poly(acrylamide) nanocomposite by varying the dosage in 50 ml of the dye solution. The removal efficiency increased from 78.16% to 83.00% upto 0.15 g dose after which there was a gradual plateau in a decreasing manner. The initial increase may be attributed to availability of adsorption sites and the plateau and eventual decrease may be as a result of saturation of the adsorption sites. However, Qe decreased from 78.16 mg/g to 11.48 mg/g with increase in adsorbent dose. This may be attributed to overlapping of adsorbent surface sites available to EY. However, further increase in adsorbent dosage had little effect on the adsorption.

Effect of Temperature and pH

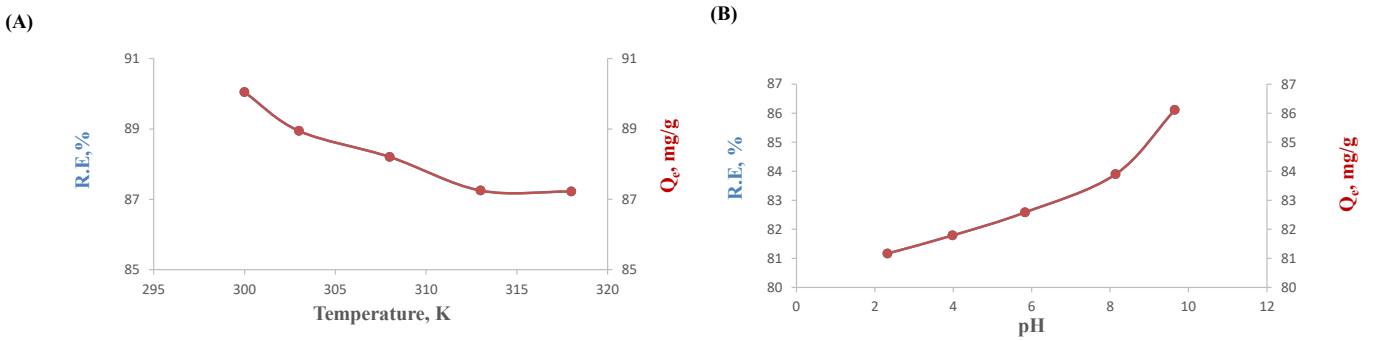

Figure 5: Effect of temperature (A) and pH (B) on EY adsorption onto FeS/chitosan-g- poly(acrylamide) nanocomposite. Conditions: (A. concentration: 100 mg/L; time: 30 minutes; dose; 0.05 g/50 ml) (B. temperature: 300 K; Time: 120 minutes; concentration: 100 mg/L).

The decrease in Qe and R.E (Fig 5A) with increasing temperature indicate that the adsorption was an exothermic process. This may be due to a decrease in adsorptive forces between the adsorbate and the adsorbent as the temperature increased.

The amount of dye adsorbed per unit mass and removal efficiently of EY were strongly affected by the pH of the wastewater as shown in Fig 5B. Qe and R.E increased gradually. This may suggest that there was a higher affinity between the adsorbate and the nanocomposite at higher pH.

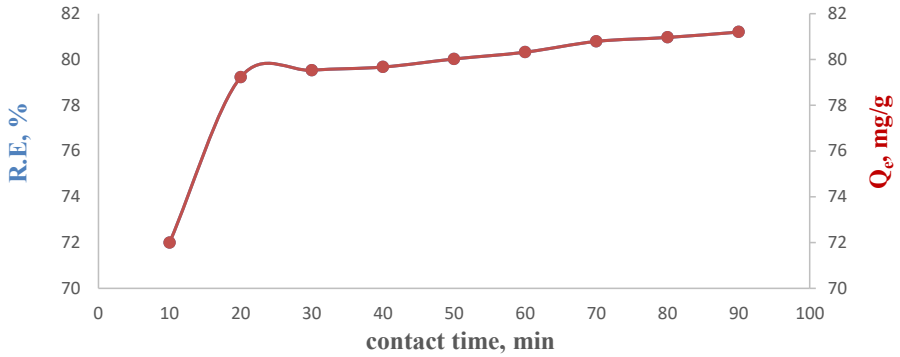

Figure 6: Effect of contact time on EY adsorption onto FeS/chitosan-g- poly(acrylamide) nanocomposite. Conditions: (concentration: 100 mg/L; dose; 0.05 g/50 ml; temperature: 300 K)

The overall trend for both R.E and Qe was the same. There was a rapid rise in adsorption between the first 10 to 30 minutes after which there was a gradual rise. The rapid rise in the first 30 minutes may be due to availability of more vacant adsorption sites.

Adsorption Isotherms

To be able to efficiently utilize the adsorption system for practical applications, it is necessary to carry out adsorption isotherm studies based on various models. Thus, the Langmuir, Freundlich and the Dubinin-Radushkevich isotherms were employed in this work.

Figure 7 below shows the isotherm equilibrium data points for adsorption of EY onto FeS/chitosan-g- poly(acrylamide) nanocomposite.

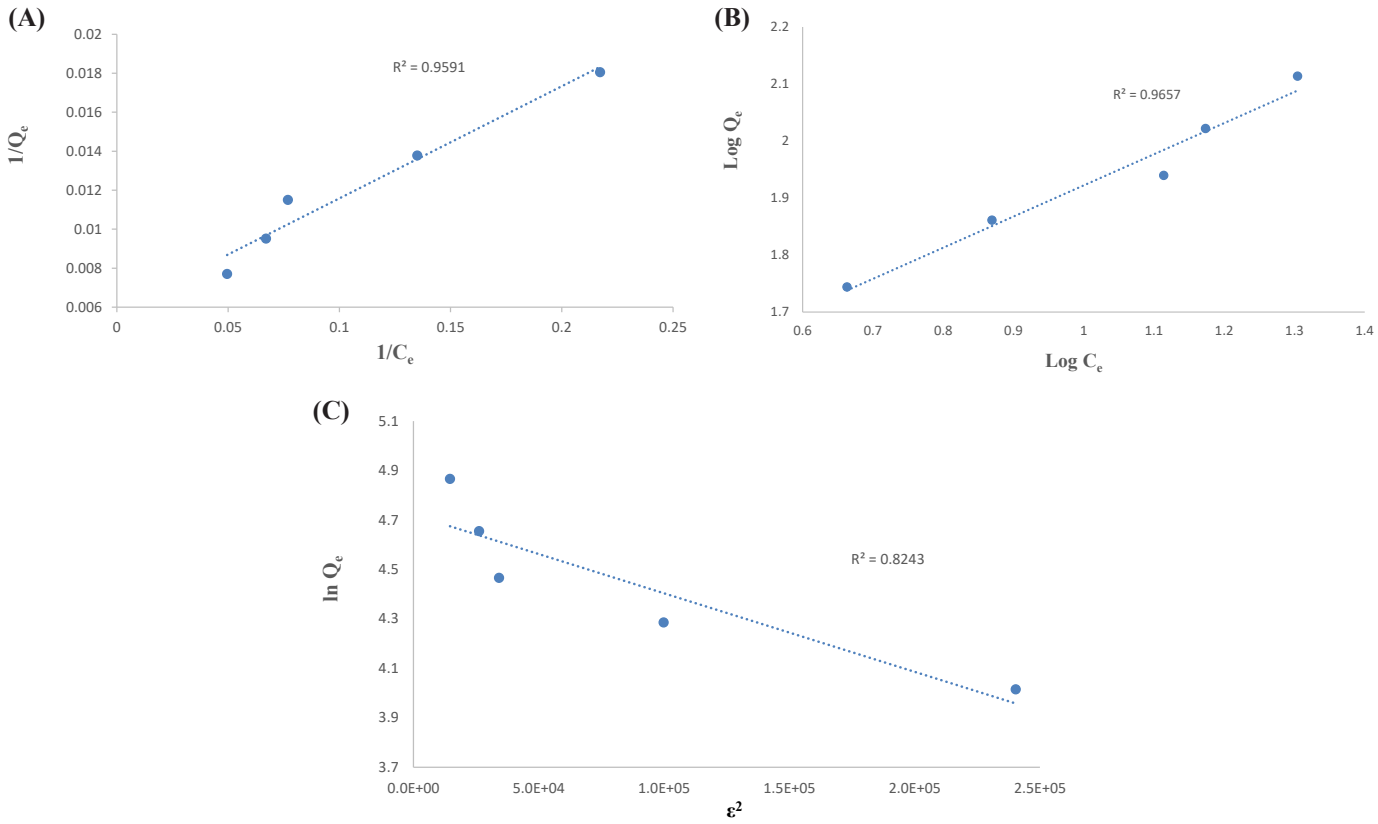

Figure 7: Langmuir (A), Freundlich (B) and Dubinin-Radushkevich (C) plots of EY adsorption onto FeS/chitosan-g- poly(acrylamide) nanocomposite.

From the graphs, the R^2 value of the Langmuir isotherm was 0.9591, Freundlich isotherm was 0.9657 and that of Dubinin-Radushkevich was 0.8243. It can be concluded that Freundlich isotherm fitted the system since the R2 value was high.

The mean free energy of adsorption, E, was found to be 0.408 kJ/mol which was within the range of $0 < E < 8$ kJ/mol thus the adsorption was physical in nature.

Adsorption Kinetics and Thermodynamic studies

In order to ascertain which kinetic order explains the adsorption of Eosin yellow onto FeS – chitosan-g- acrylamide composite, the contact time studies were analyzed using the pseudo-first-order and the pseudo-second-order kinetics. The best fit results were obtained in the pseudo-second-order model with an R^2 value (0.9997) closer to unity as compared to the pseudo-first-order R^2 value of 0.9673. Hence, it was established that the adsorption followed a pseudo-second-order process. A similar trend on the adsorption of Eosin Y was reported by [6,14].

Table 1 below summarizes the thermodynamic studies of the adsorption process

Table 1: Thermodynamic parameters for EY adsorption onto FeS/chitosan-g-poly(acrylamide) nanocomposite

ΔH°(kJ/mol)	ΔS°(kJ/mol)	ΔG°(kJ/mol.K)				
		300 K	303 K	308 K	313 K	318 K
-12.243	-0.023	-5.492	-5.252	-5.152	-5.005	-5.078

The negative ΔHo value indicated an exothermic process which correlates to the adsorption studies on the effect of temperature on the adsorption process. The negative value of ΔSo showed a reduced randomness during the adsorption process. The negative values of ΔGo suggested spontaneity of the adsorption process.

Conclusion

FeS and FeS/chitosan-g-acrylamide nanomaterials were successfully synthesized by co-precipitation and microwave assisted grafting respectively. The XRD spectra confirmed the tetragonal phase of FeS and particle size within the nanometer range. The FTIR confirmed the formation of FeS and its associated nanocomposite.

SEM and TEM confirmed the morphology of the nanoparticle as well as the grafting of the polymers (chitosan and acrylamide). The SAED pattern gave an indication of the polycrystalline nature of the nanoparticle. Batch adsorption studies revealed the dependency of the nanomaterial on adsorbent dosage, pH, temperature, contact time and adsorbate concentration. The Freundlich isotherm model fitted the adsorption process. This is an indication of a heterogenous adsorption. The thermodynamic parameters according to the ΔG° showed a spontaneous and thermodynamically stable process, the ΔS° gave an indication of a reduced disorderliness in the adsorption process and the ΔH° revealed that the adsorption process was exothermic. The FeS/chitosan-g-acrylamide therefore showed potential use as an adsorbent for the removal of organic dyes (Eosin Y) from wastewater.

Acknowledgements

The authors acknowledge Mr. Ebenezer Adom and Mr. Ernest Sintim, Chemical Engineering Department of KNUST, Mr. Nana Gyasi, Ms Naomi C. Kabiri and Mr. Kingsley Adukpoh, Chemistry Department of KNUST for their technical support.

The authors also acknowledge the support from DST-CSIR National Center for Nanostructured Materials, CSIR for the characterization of the materials and the support of the Royal Society-DFID ACBI towards this work [33,38].

References

1. Ali, M., & Sreekrishnan, T. R. (2001). Aquatic toxicity from pulp and paper mill effluents: a review. Advances in environmental research, 5(2), 175-196
2. Pokhrel, D., & Viraraghavan, T. (2004). Treatment of pulp and paper mill wastewater—a review. Science of the total environment, 333(1-3), 37-58
3. Mahmoodi, N. M., & Arami, M. (2008). Modeling and sensitivity analysis of dyes adsorption onto natural adsorbent from colored textile wastewater. Journal of Applied Polymer Science, 109(6), 4043-4048..
4. Mahmoodi, N. M., & Arami, M. (2009). Degradation and toxicity reduction of textile wastewater using immobilized titania nanophotocatalysis. Journal of Photochemistry and Photobiology B: Biology, 94(1), 20-24.
5. Mahmoodi, N. M., & Arami, M. (2009). Numerical finite volume modeling of dye decolorization using immobilized titania nanophotocatalysis. Chemical Engineering Journal, 146(2), 189-193.
6. Subramani, S. E., & Thinakaran, N. (2017). Isotherm, kinetic and thermodynamic studies on the adsorption behaviour of textile dyes onto chitosan. Process Safety and Environmental Protection, 106, 1-10
7. Chatterjee, S., Chatterjee, S., Chatterjee, B. P., Das, A. R., & Guha, A. K. (2005). Adsorption of a model anionic dye, eosin Y, from aqueous solution by chitosan hydrobeads. Journal of colloid and interface science, 288(1), 30-35.
8. Gupta, K., Bhattacharya, S., Chattopadhyay, D., Mukhopadhyay, A., Biswas, H., Dutta, J., ... & Ghosh, U. C. (2011). Ceria associated manganese oxide nanoparticles: synthesis, characterization and arsenic (V) sorption behavior. Chemical Engineering Journal, 172(1), 219-229.
9. Aksu, Z. (2005). Application of biosorption for the removal of organic pollutants: a review. Process biochemistry, 40(3-4), 997-1026.
10. Fosso-Kankeu, E., Mittal, H., Mishra, S. B., & Mishra, A. K. (2015). Gum ghatti and acrylic acid based biodegradable hydrogels for the effective adsorption of cationic dyes. Journal of Industrial and Engineering Chemistry, 22, 171-178.]
11. Sánchez-Martín, J., Beltrán-Heredia, J., & Gragera-Carvajal, J. (2011). Caesalpinia spinosa and Castanea sativa tannins: A new source of biopolymers with adsorbent capacity. Preliminary assessment on cationic dye removal. Industrial Crops and Products, 34(1), 1238-1240.
12. Zhang, Z., O'Hara, I. M., Kent, G. A., & Doherty, W. O. (2013). Comparative study on adsorption of two cationic dyes by milled sugarcane bagasse. Industrial Crops and Products, 42, 41-49.
13. Jeon, Y. S., Lei, J., & Kim, J. H. (2008). Dye adsorption characteristics of alginate/polyaspartate hydrogels. Journal of Industrial and Engineering Chemistry, 14(6), 726-731.
14. Mittal, H., & Mishra, S. B. (2014). Gum ghatti and Fe3O4 magnetic nanoparticles based nanocomposites for the effective adsorption of rhodamine B. Carbohydrate polymers, 101, 1255-1264.
15. Zhou, Y. T., Nie, H. L., Branford-White, C., He, Z. Y., & Zhu, L. M. (2009). Removal of Cu2+ from aqueous solution by chitosan-coated magnetic nanoparticles modified with α-ketoglutaric acid. Journal of colloid and interface science, 330(1), 29-37
16. Mittal, H., & Ray, S. S. (2016). A study on the adsorption of methylene blue onto gum ghatti/TiO2 nanoparticles-based hydrogel nanocomposite. International Journal of Biological Macromolecules, 88, 66-80.
17. Xu, Y. Y., Zhou, M., Geng, H. J., Hao, J. J., Ou, Q. Q., Qi, S. D., ... & Chen, X. G. (2012). A simplified method for synthesis of Fe3O4@ PAA nanoparticles and its application for the removal of basic dyes. Applied Surface Science, 258(8), 3897-3902
18. Shukla, S. K., Mishra, A. K., Arotiba, O. A., & Mamba, B. B. (2013). Chitosan-based nanomaterials: A state-of-the-art review. International journal of biological macromolecules, 59, 46-58.
19. Hirano, S., Seino, H., Akiyama, Y., & Nonaka, I. (1990). Chitosan: a biocompatible material for oral and intravenous administrations. In Progress in biomedical polymers (pp. 283-290). Springer, Boston, MA
20. Pillai, C. K., Paul, W., & Sharma, C. P. (2009). Chitin and chitosan polymers: Chemistry, solubility and fiber formation. Progress in polymer science, 34(7), 641-678.
21. Park, D., Yun, Y. S., & Park, J. M. (2010). The past, present,

and future trends of biosorption. Biotechnology and Bioprocess Engineering, 15(1), 86-102.
22. Park, Y. K., & Lee, C. H. (1996). Dyeing wastewater treatment by activated sludge process with a polyurethane fluidized bed biofilm. Water Science and Technology, 34(5-6), 193-200.
23. Gupta, D., Singh, D., Kothiyal, N. C., Saini, A. K., Singh, V. P., & Pathania, D. (2015). Synthesis of chitosan-g-poly (acrylamide)/ZnS nanocomposite for controlled drug delivery and antimicrobial activity. International journal of biological macromolecules, 74, 547-557.
24. Freundlich H (1907) About adsorption in solutions. Journal of Physical Chemistry 57: 385-470.
25. Dubinin, M. M. (1947). The equation of the characteristic curve of activated charcoal. In Dokl. Akad. Nauk. SSSR. (Vol. 55, pp. 327-329).
26. Kaur, G., Singh, B., Singh, P., Singh, K., Thakur, A., Kumar, M., ... & Kumar, A. (2017). Iron disulfide (FeS2): a promising material for removal of industrial pollutants. ChemistrySelect, 2(6), 2166-2173.
27. Malek, T. J., Chaki, S. H., & Deshpande, M. P. (2018). Structural, morphological, optical, thermal and magnetic study of mackinawite FeS nanoparticles synthesized by wet chemical reduction technique. Physica B: Condensed Matter, 546, 59-66.
28. Pathania, D., Gupta, D., Ala'a, H., Sharma, G., Kumar, A., Naushad, M., Ahamad, T. and Alshehri, S. M. (2016). Photocatalytic degradation of highly toxic dyes using chitosan-g-poly (acrylamide)/ZnS in presence of solar irradiation. Journal of Photochemistry and Photobiology A: Chemistry, 329, 61-68.
29. Gong, Y., Liu, Y., Xiong, Z., Kaback, D., & Zhao, D. (2012). Immobilization of mercury in field soil and sediment using carboxymethyl cellulose stabilized iron sulfide nanoparticles. Nanotechnology, 23(29), 294007.
30. Kim, E. J., Kim, J. H., Azad, A. M., & Chang, Y. S. (2011). Facile synthesis and characterization of Fe/FeS nanoparticles for environmental applications. ACS applied materials & interfaces, 3(5), 1457-1462.
31. Pethkar, A. V., & Bhagat, A. P. (2013). Biopolymer stabilized iron sulphide nanoparticles for removal of acid black 1 dye. In Materials Science Forum (Vol. 757, pp. 285-293). Trans Tech Publications Ltd.
32. Gartman, A., Findlay, A. J., & Luther III, G. W. (2014). Nanoparticulate pyrite and other nanoparticles are a widespread component of hydrothermal vent black smoker emissions. Chemical Geology, 366, 32-41.
33. Egerton, R. F. (2005). Physical principles of electron microscopy (Vol. 56). New York: Springe
34. Langmuir, I. (1916). The constitution and fundamental properties of solids and liquids. Part I. Solids. Journal of the American chemical society, 38(11), 2221-2295.
35. Mahmoodi, N. M., Salehi, R., Arami, M., and Bahrami, H. (2011). Dye removal from colored textile wastewater using chitosan in binary systems. Desalination, 267(1), 64-72
36. Mittal, A., Jhare, D., & Mittal, J. (2013). Adsorption of hazardous dye Eosin Yellow from aqueous solution onto waste material De-oiled Soya: Isotherm, kinetics and bulk removal. Journal of Molecular Liquids, 179, 133-140.
37. Paca, A. M., & Ajibade, P. A. (2018). Synthesis, Optical, and Structural Studies of Iron Sulphide Nanoparticles and Iron Sulphide Hydroxyethyl Cellulose Nanocomposites from Bis-(Dithiocarbamato) Iron (II) Single-Source Precursors. Nanomaterials, 8(4), 187
38. Shaw, C. B., Carliell, C. M., & Wheatley, A. D. (2002). Anaerobic/aerobic treatment of coloured textile effluents using sequencing batch reactors. Water research, 36(8), 1993-2001.